Tutor/s

Dr. Ramón Reigada Sanz
Departament de Ciència de Materials i Química Física

Grau de Química

Treball Final de Grau

Molecular Dynamics study of the effect of graphene on lipid bilayers.

Estudi amb Dinàmica Molecular de l'efecte del grafè sobre bicapes lipídiques

Raul Santiago Piera

June 2017

Universitat de Barcelona

B:KC Barcelona Knowledge Campus
Campus d'Excel·lència Internacional

Aquesta obra esta subjecta a la llicència de:
Reconeixement–NoComercial-SenseObraDerivada

http://creativecommons.org/licenses/by-nc-nd/3.0/es/

La Física és massa important per ser deixada als físics.

David Hilbert

Primerament, m'agradaria agrair al Ramón per tota l'ajuda durant el treball i per la enorme quantitat i qualitat de consells i coneixement que m'ha aportat. També m'agradaria agrair la Cristina, l'Alberto i el Toni per totes aquestes hores que m'han dedicat duran aquests mesos, tant a nivell personal com professional. Per últim, vull donar les gràcies a l'Anna per encoratjar-me a seguir endavant i motivar-me quan més ho he necessitat.

REPORT

CONTENTS

1. SUMMARY

The interaction of graphene-based materials with cells has recently become an important field of study. Its relevance lies on the demonstrated graphene toxicity for the human beings.

In this project, the graphene effect on lipid vesicles (the simplest model of cell membrane) is studied by means of coarse-grained Molecular Dynamics. Different simulations have been performed in order to track the evolution path between both graphene and graphene oxide with an interacting vesicle. Moreover, POPC and cholesterol are chosen to compose the vesicle. Three different variables have been taken into account: oxidation degree, size, and relative orientation of the graphene sheet.

First, two different graphene oxidation states have been considered (0% and 20%). For each of those, both large and small graphene sheet sizes have been built. These four specific graphene sheets have been placed in four relative orientations with respect to the lipid vesicle, labelled as corner, edge, face, and inside initial positions. This set of initial conditions appears to affect the system evolution path, registering 6 different outcomes out of 16 simulations.

Analysis of the MD results reveals useful information about the effects of graphene size, oxidation and orientation and it also helps to register some synergies between them. For example, the relative orientation effect appears to determine the final system configuration in larger graphene sheets. In turn, it does not appear to be relevant in the small-sized cases. On the other hand, the relative oxidation seems affect in the evolution path independently of the size. Moreover, the vesicle curvature effect has been also noticed by comparing the lasting final state of some graphene-lipid vesicle simulations with respect to considering a planar lipid bilayer. Finally, a graphene-mediated vesicle fusion is registered on placing two identical vesicles in direct contact with a large graphene sheet.

Keywords: Coarse-grained Molecular Dynamics, lipid vesicle membrane, graphene, graphene oxide, POPC, cholesterol, vesicle, liposome.

2. RESUM

La interacció dels materials basats en el grafè amb cèl·lules s'ha tornat, recentment, en un camp molt estudiat. La seva rellevància radica en la demostrada toxicitat de les nanopartícules de grafè per las éssers vius.

En aquest projecte s'estudia el efecte del grafè sobre vesícules lipídiques (el models més senzills de membrana cel·lular) mitjançant la Dinàmica Molecular de gra gros. S'han fet diferents simulacions amb la intenció de realitzar un seguiment en el patró d'interacció entre el grafè, i el òxid de grafè, amb una vesícula composta de POPC i colesterol. En les simulacions, s'han controlat tres variables diferents: el grau d'oxidació, la mida i la orientació relativa del grafè respecte la vesícula.

En primer lloc, s'han considerat dos estats d'oxidació diferents pel grafè (0% i 20%). Per cadascun d'aquests, s'han construït fulles de grafè de una mida gran i petita. Les quatre fulles s'han col·locat en diferents posicions relatives que pot prendre el grafè respecte la vesícula, etiquetades com de costat, de vèrtex, de cara o dintre de la vesícula. Aquest conjunt de variables sembla afectar al la ruta en la que el sistema evoluciona, ja que s'han enregistrat 6 dinàmiques diferents de les 16 simulacions realitzades.

L'anàlisi de les simulacions ha revelat dades útils sobre l'efecte de les condicions d'interacció i ajuda a observar sinèrgies entre elles. Per exemple, l'efecte de la posició relativa sembla determinar la configuració final per fulles de grafè grans, però, no sembla afectar en fulles petites. En canvi, la oxidació del grafè sembla influir independentment de la resta de variables. Per altre banda, l'efecte en la curvatura vesicular s'ha pogut observar en comparar el estat final les simulacions respecte al obtingut en considerar una bicapa lipídica plana. Finalment, s'ha detectat una fusió de vesícules catalitzada per la presència del grafè entre dues vesícules idèntiques.

Paraules clau: Dinàmica Molecular de gra gros, membrana lipídica, grafè, òxid de grafè, POPC, colesterol, vesícula, liposoma.

3. INTRODUCTION

3.1. PRECEDENTS

Nowadays, many research fields are focused on the study of carbon-based nanomaterials, such as graphene sheets, graphene nanotubes and fullerene. The graphene applicability ranges go from biomedical engineering to the development of large-surface electro-catalytic devices. All those nanomaterials have become widely used since a cheap graphene synthetic method was developed. Graphene is not only one of the strongest materials known but it also presents electronic conductivity characteristics [1]. These properties lie on the atomic structure of graphene monolayer. A 2D hexagonal lattice with only sp^2 hybridization carbon atoms forms it, each of those hosting an unpaired electron and creating a delocalized π-cloud.

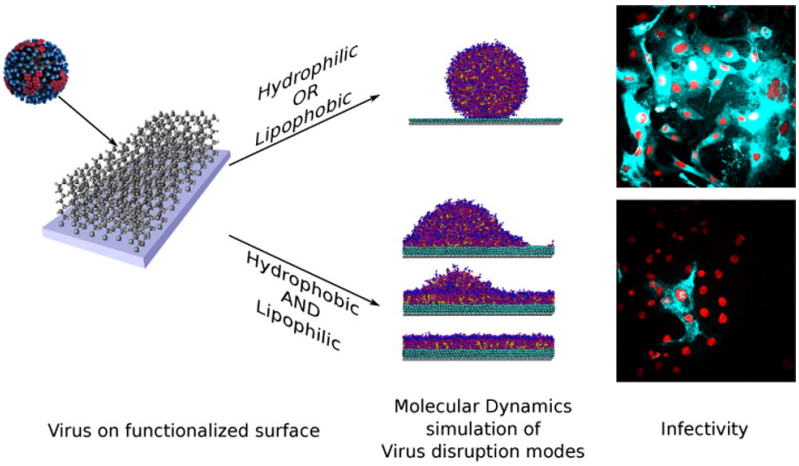

Figure 1. It is shown how the tailored apolar surfaces can reduce the biological activity of a virus colony. The virus interact with supported hydrophobic material and spreads on the surface. As it is shown in the right panels, the infectivity decreases. (Image from Mannelli et al. Ref 4)

Even its useful applications, graphene-based materials have also some inconveniences. It can be spread out as a nanoparticle and it can be found suspended in the air coming, for example, from industry wastes. As a consequence, it can be inhaled and introduced to the human body. This fact is supported by studies [2], which demonstrate the presence of graphene particles in different tissues, including the lungs. Moreover, recent scientific research focused on the study of the interaction between carbon-based nanomaterials with cells appeared. These studies show that the extended graphene surfaces, like many other tailored apolar surfaces [3,4], could strongly interact with the apolar tails of the lipids of a planar lipid bilayer [5] or a membrane of bacterial cell [6-8] (Figure 1). This causes a change in their biological activity, killing them and acting as antibacterial. The potential harmfulness lays on the fact that, graphene and its derivatives, cannot only interact with bacterial cells but also with eukaryote ones.

Other carbon-based nanomaterials, that are even more harmful than graphene, are its oxide derivatives [9,10], which exhibit significant solubility in aqueous media. Graphene oxides are chemically formed by the covalent interaction of two carbon atoms with oxygen one, forming an epoxy bond [11]. Since graphene sheets can be very extended, the epoxy bond formation can take place multiple times along the lattice. Therefore, a large set of graphene oxides could be potentially found according to its atomic topology and oxidation degree. The graphene oxide toxicity for human beings has been experimentally demonstrated. However, there is still research to do on how graphene, or its oxides, interact with cells. Therefore, an understanding of cell-graphene interaction mechanism must be provided.

3.2. CELL MEMBRANE AND LIPOSOME SIMPLIFICATION

The biological shape of eukaryote cells can be described as cytoplasm and water nesting a large number of supra-molecular complexes such as ribosomes, mitochondria or the nuclei, as many other organelles. The cytoplasm is wrap together by the cellular membrane, which recovers and protects the entire cell. Therefore, the very first interaction between eukaryote cells and graphene must take place through the membrane, which might be the first studied interaction.

Cell membranes are biological walls that separate the inner part of the cell from its environment. They are constituted by large number of amphipathic lipids with different chemical natures, forming a bilayer. This membrane is decorated with proteins that are involved in cell

recognition or substances transfer and many other processes. The membrane lipids are commonly phospholipids that form a bilayer configuration. The phospholipid's polar heads are arranged in contact with water and the apolar tails meshed together in the inner part, far from the polar solvent. This configuration is energetically favourable compared to the solvated state because it minimizes both surface area and polar-apolar interactions. The membrane composition is widely complex, due to this, it would be difficult to obtain a clear molecular detail form simple experiments. If the lipids are the system of interest, a spherical lipid bilayer might be taken as the simplest model of cell, which is commonly called a vesicle liposome.

3.3. PROJECT STUDY

In this work the liposome-graphene interaction will be inquired by means of the molecular dynamics approach. The study will be focused on the qualitative analysis of the different interaction modes between liposome and graphene that could appear by changing some conditions on the simulated contact.

Some computational works reported [12-14] that, for plane lipid bilayers surrounded by water, graphene-bilayer interaction dynamics vary depending on the initial orientation of the graphene sheet with respect to the lipid plane. Moreover, it is possible that both final state equilibrium conformation and dynamics change depending on the oxidation degree of the graphene sheet. Finally, when dealing with non-planar vesicle bilayers, it could also be affected by the relative size of the graphene layer with respect to the contacting vesicle. For this reasons those previously mentioned parameters are investigated in this work.

4. OBJECTIVES

The scope of this work is to provide a qualitative explanation of the graphene-lipid bilayer interaction by Molecular Dynamics simulations.

To analyse the graphene-vesicle interaction models depending on the following aspects:

a) The initial position of the graphene sheet respect to the vesicle
b) The oxidation degree of the graphene sheet
c) The size of the graphene sheet

To compare the different behaviour of the graphene over the lattice depending on whether the lipid bilayer is curved or it is planar.

To analyse the catalytic effects of graphene sheets with respect to vesicle fusion phenomena.

5. COMPUTATIONAL DETAILS

The core study in this project consists on performing time-dependent simulations of graphene-lipid bilayer interactions. One of many possible options choses to perform those simulations is the MD technique. In this section, the basic fundamentals of the MD approach are established. Moreover, the specifications of the software and force fields used for the project are listed.

5.1 MOLECULAR DYNAMICS APPROACH

Molecular modelling is one way to describe complex chemical systems in terms of the better possible particle resolution. The main goal is to predict the macroscopic properties of a given system of interacting particles obtaining such properties from a statistical mechanics treatment of the microscopic ones. Nowadays, there exist basically two methods for the time-dependent calculations computationally reachable from a simulation point of view: Monte Carlo methods and Molecular Dynamics. The Monte Carlo methods loose the molecular description of the simulated particles but it improves the simulation time expense. Therefore, it is sometimes inadequate for the description of the microscopic detail, generally required to explain changes at the molecular scale. On the other hand, Molecular Dynamics keeps the molecular detail but the computation of the forces acting on every atom, or atom group, is required. Additionally, an obvious advantage of MD over MC is that it provides a correct description of the dynamics of the simulated system, not only in the equilibrium state. In this work the Molecular Dynamics method is used, because the particle nature and molecular detail is needed to describe the interacting processes.

There exist several techniques in order to solve the Molecular Dynamics equations. The chose of the technique depend on the simulation aim and on the reliability of the results inherent to the method. Ideally, the quantum MD equation provides the best accuracy but when the number of simulated particles gets big it is usually unreachable to solve from a computational point of view. Thus, to compute larger and more complex systems some approximations are needed. One of the commonly used simplifications is based on considering classical MD instead

of quantum MD. Nevertheless, it won't be possible depending on the studied system. For example, considering quantum MD makes possible to describe chemical reactions, and this is unreachable by the use of classical MD simulations. On the other hand, longer simulation times can be reached and processes at the microsecond scale could be studied by means of the classical MD. Then, the method's chose will be restricted to the system's complexity, total number of particles, required accuracy for the simulation and also on the simulation aim. Essentially, a solution to it would be the best compromise between the chemical accuracy and the time invested for the simulation. In Figure 2, a large amount of simulation methods are exposed and classified according to the timescale of the study and length-scale of the simulated system. In this case, classical and coarse-grained MD is the appropriate method.

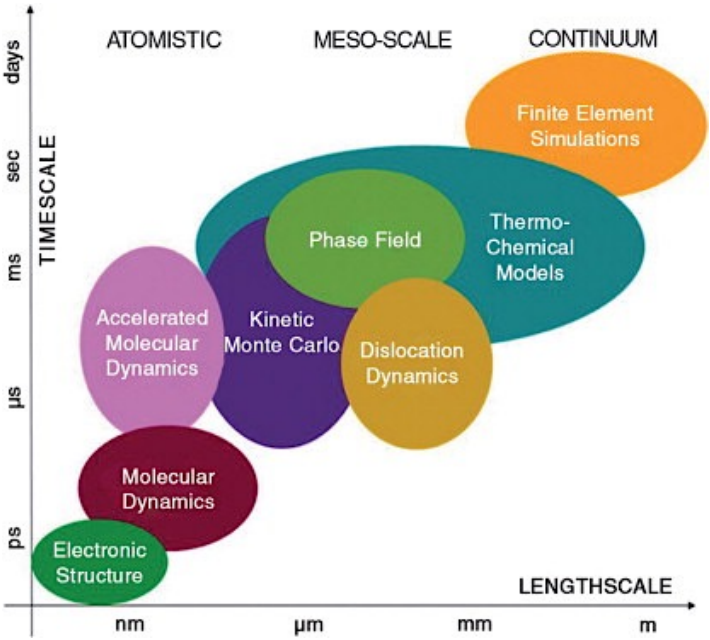

Figure 2. Appropriate simulation methods depending on the timescale and the length-scale of the simulated system. As the time and system size decrease, more precise simulations can be performed. *(Extracted from Stan, M. Discovery and Design of Nuclear Fuels. Materialstoday **2009,** 12, 20-28)*

The Molecular Dynamics approach consists on solving the Newton's equation of motion for a system of interacting particles.

$$m_i \frac{\partial^2 r_i}{\partial t^2} = F_i$$

The forces acting on each particle are simultaneously calculated as the derivative of the potential energy function of the particle with respect to its position.

$$F_i = -\frac{\partial V}{\partial r_i}$$

Numerically solving this system of equations, and imposing a certain time-step, make possible to calculate the positions of each particle in the next step. The general Molecular Dynamics algorithm is summed up in Figure 3.

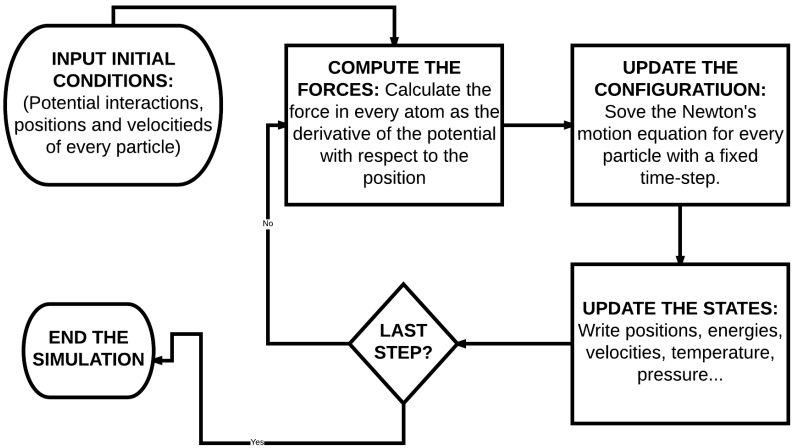

Figure 3. Numerical algorithm for the MD simulations. A loop process is performed until the last simulation step is achieved.

5.3. FORCE FIELDS AND MARTINI COARSE-GRAINING

A force field is an empirical parameterization of the different particle interactions existing on a particle system. The parameters of the force field are consistently optimized fitting to the macroscopic data extracted from the simulation to the experimental results. There exist two different force field interactions according to the nature of the coupled particles: bonded

interactions and non-bonded interactions. In Figure 4, there is a summary of all the possible ones.

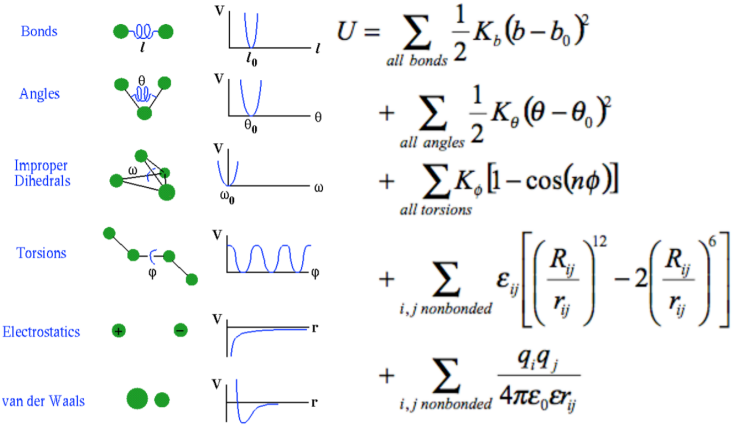

Figure 4. All the possible interactions in the force field simplification. From left to the right: Interaction name, schematic representation, function shape and analytical expression. The first four interactions belong to the intramolecular setting and the other belongs to the intermolecular one.

Bonded interactions collect the covalent bond stretching, the angle bending, proper dihedrals and improper dihedrals. Basically it is the subdivision that considers all the intra-molecular potentials. Again, there exist many parameterization functions for any of the bonded interactions. In this case, the harmonic oscillator approach is considered for each of them. The harmonic oscillator could be compared with the common Hooke equation. In this case, the parameterized values would be the spring constant and the equilibrium position. For the non-bonded particles, Van der Waals interactions are modelled by typical Lennard-Jones potential, whereas electrostatic interactions are derived by the Coulomb potential.

According to the force field parameterization, there is no restriction of how the particles in the simulation have to be defined. Thus, every simulated particle could be taken as a bead that includes more than one real particle. This approximation is called **Coarse-Grained Molecular Dynamics** (CGMD). Although the particles could be defined freely, they must be set maintaining physical meaning and also with a solid force field parameterization beyond (See Figure 2).

In this project, the MARTINI force field [15] is the ones used. It use a parameterization based on a 4-to-1 coarse-grain mapping, and 3-to-1 for the cyclic molecules. This notation means that every coarse-grain bead include 4 real atoms, excluding hydrogen. The MARTINI

force field beads are conveniently defined by two factors: polarity and acid-base characteristics of the particle. On the one hand, the particles are split in four different groups according to its polarity. Particles are tagged as polar (P), non-polar (N), apolar (C) or charged (Q) depending on its behaviour. For the cyclic particles a prefix (S) is appended to the particle definition. On the other hand, particles are subdivided in donor (d), acceptor (a), both (da) or none (0) according to the acid-base characteristics. Moreover, in the charged particles case, a 1-5 scale is used to indicate the polarity degree. The simulated molecules in the studied system are POPC, cholesterol, graphene and graphene oxides. According to the MARTINI force fields, the coarse-grained molecules are the ones shown in Figure 5.

In lipids and water coarse-grained particles the parameterization has been widely tested. However, in the graphene case, there is still being refined. There are a large number of graphene force fields conveniently parameterized in the literature according to the MARTINI context. In this work the one described in [16] and represented in Figure 5 it is used because reproduces sort of the properties of graphene, such as stiffness, flexibility and many other properties.

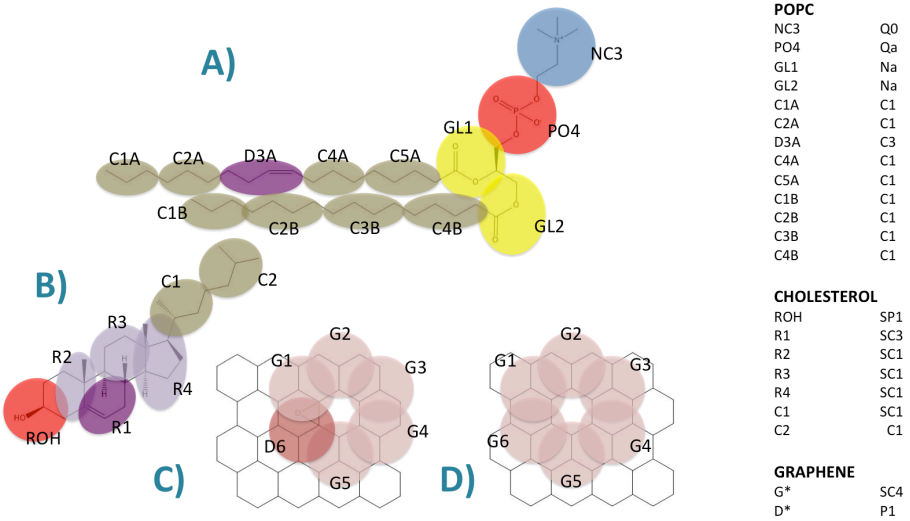

Figure 5. The coarse-graining of the different molecules used, according to the MARTINI parameterization. A) POPC, B) cholesterol, C) graphene oxide, D) graphene. Left-hand of the image: particle definitions for all the molecules.

5.4. STUDIED CONDITIONS

In this section, the molecules used in the simulations and the simulation conditions are described. First the vesicle composition is determined. In order to make the simulation as much consistent as possible with biological conditions, POPC and 30% of cholesterol lipids will be used in the simulations. Those two lipids are commonly found in eukaryote cell membranes. POPC is an unsaturated phospholipid, whose polar head is composed by a phosphate liked to a choline group. The fluid properties of this vesicle allow POPC to move along the lipid bilayer but flip-flop movement between leaflets the simulation time scale (Figure 6, top). On the other hand, cholesterol is a polycyclic organic molecule with also a polar head, a hydroxyl group. As it exhibits a rather planar shape, it is understood to reduce the in-plane membrane movement by compacting the rest of lipids present. Besides, the cholesterol flip-flop movement is observed at the simulation time scales (Figure 6, bottom) because it is smaller and the kinetics is highly favourable, being compared to POPC. All these features reproduces quiet well the properties of a typical eukaryotic cell membrane. In all the simulations the vesicles is built with 614 POPCs and 263 cholesterol molecules. In the vesicle rearrangement it is translate to 12nm vesicle long.

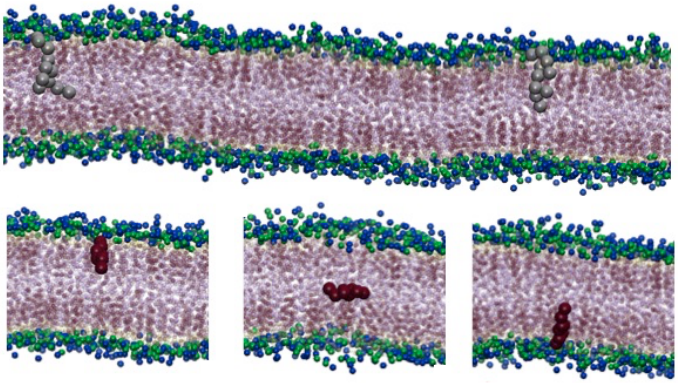

Figure 6. Representation of a planar cell membrane. Top: A coarse-grained POPC molecule is plotted in grey. Bottom: cholesterol is plotted in red. POPC moves along the surface direction whereas cholesterol flip-flops to the lower layer. Colour code: Blue: NC3 (choline); Green: PO4 (phosphate); Purple (POPC tails and cholesterol)

On the other hand, there are a wide number of different relative orientations that graphene can take with respect to a lipid vesicle. All the possible configurations could be reduced to four

different limit ones: corner, face, edge and inner contact. In Figure 7, there are collected the different limit configurations that will be used as a starting point for the MD calculations.

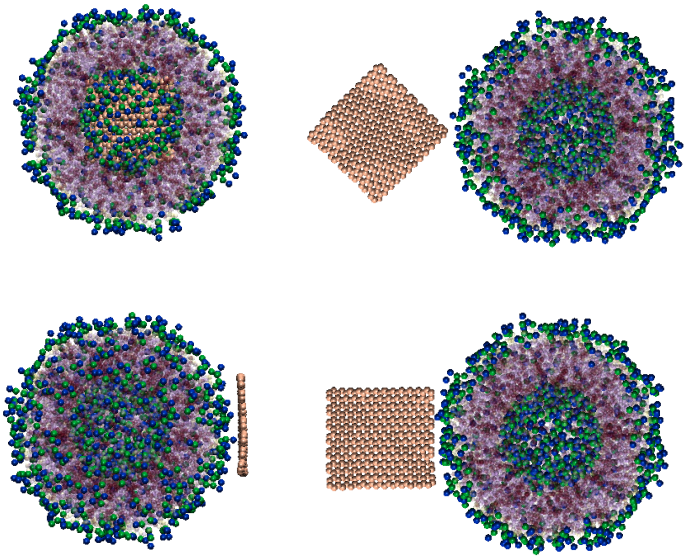

Figure 7. All the different initial settings used for the MD simulations. Top-left: inside, top-right: corner, bottom-left: face, bottom-right: edge. In this case, the graphene sheet represented in the picture is built using a 12x13 coarse-graining. The small graphene sheets initial setting is almost equal to the ones represented here.

According to the graphene size, two different graphene sheets are built, large and small one. The large-size graphene is built with 12x13 coarse-grained beads. Its area is 36nm^2 and keeps a 3:2 linear relation with respect to the vesicle radius. For this reason, this graphene size is considered particularly big. On the other hand, the other graphene sheet is several times smaller and keeps a 1:4 linear relation with respect to the vesicle. In this case its area is 4nm^2. The small graphene sheet is built by 4x5 coarse-graining.

Moreover, the oxidized graphene sheets are built by randomly substituting 20% of the coarse-grained beads for ones that simulate an epoxidised particle. The random setting does not affect to the simulation outcomes, because for every simulation the same oxidation topology is maintained. Notice the different polarity of the substituted particles according to graphene with respect to graphene oxide (GO) in Figure 5.

There exist many other parameters that might affect to the possible interaction modes such as temperature, pressure or the vesicle curvature. Those parameters have been also set in order to properly imitate the biological conditions. Then, pressure and temperature are set to 1 bar and 310K, respectively, taking water as the solvent. Finally, the vesicle curvature has been fixed by performing every simulation at constant number of lipid particles.

5.5. OTHER COMPUTATIONAL DETAILS

In this section other simulation specifications will be explained. Unlike the previous one, this will be focused on the simulation conditions but not on the methods and molecule specifications. First of all, it is important to highlight that the coarse-grained MD simulations will be performed using the GROMACS software [17]. All computational details explained in this section, and in the previous ones, are supported by the GROMACS version 4.5.4.

5.5.1. Energy minimization

The energy minimization final goal is to find the closest local potential energy minima coordinates for any particle of the system [18]. There exist many numerical methods in order to find local minima but the implementation of those is out of the scope of this project. This procedure it is commonly useful after the handmade initial topologies are built. Using FORTRAN codes, a particle system could be roughly moved to an untrue configuration close to the real one. It is common that, if one performs a simulation with handmade configurations, couples of atoms might be too close and, by solving the motion Newton's equations, the computed forces could be unreasonably big. Therefore, an energy minimization calculation is always done before starting the MD simulation to avoid this problem.

5.5.2. Periodic Boundary conditions

The simulation box is an important feature to consider because it influences on what is surrounding the simulated particle system. There exist two main ways to describe the particle interaction with the box limits. The first one consists on taking the system as if it was isolated. In this approach, particles stumbling upon the walls elastically scatters without energy exchange. Conversely, there exist the possibility to periodically repeat the unit cell in all three dimensions, so called periodic boundary conditions (PBC). In this case, if a particle pass trough the box side it re-appears in the opposite box side with the same velocity. PBC are used in this work

because it provides the system with chemical context. Nevertheless, the number of the required computed forces exponentially reach with this method. In order to control this fact, a radial cut-off distance is set for every particle.

5.5.3. Freezing of water

The Coarse-grain-based methods have a set of limitations. In this work case of interest, is possible to face simulations where water freezes around 300K when it is in direct contact with a graphene sheet. This phenomenon takes place because grouping atoms decrease the degrees of freedom of the system experimenting an entropy decree. Thus, some thermodynamic constants, such as the freezing temperature are shifted. Nevertheless, there exist some tricks in order to overcome these problems and reducing the consequences. One of the different possibilities is to substitute a given percentage of waters by “anti-freezing” ones. These last waters have the same force field parameters but its thickness is slightly bigger. Its effect lies on the inhibition of the crystalline ice formation due to greater volume of the anti-freezing waters, which makes the ice clustering energetically higher, so that, more improbable. In this work, a 15% of anti-freezing water is included on the simulations to avoid this problem.

5.5.4. Ensemble, thermostats and barostats

There exist a lot of proper ensembles, in the statistical thermodynamics context, useful to predict the macroscopic data from the simulation. In this work, all the simulations are performed in the isothermal-isobaric ensemble. This specific ensemble suits perfectly the simulation context because it fixes the total number of particles, temperature and pressure. Then, the control of these variables during the simulations is required. MD method does not intrinsically fix the conditions although exist algorithms in order to have this variables properly controlled, computational thermostats and barostats. In all the simulations performed in this work the Berendsen thermostat and barostat have been used. In Table 1, there are collected all the important conditions for the MD simulations.

FIXED CONDITION	SIMULATION VALUE
Number of POPC molecules	614 (70%)
Number of cholesterol molecules	263 (30%)
Number of water particles	61552
Vesicle diameter	12 nm
Graphene size	36nm^2(large) and 4nm^2(small)
Graphene oxidation degree	0% and 20%
Graphene relative orientation	Corner, edge, inside, face
% Anti-freezing waters	15%
Total simulation time	1000 ns
Simulation time-step	0.2 ps
Pressure and temperature	1 bar (Berendsen) and 310K (Berendsen)

Table 1: Values of the most important parameters for the MD calculations.

6. RESULTS

In this section, the MD performed for all the simulation sets are shown. The description of the results is split in four different sections, which respectively contains all the combinations between graphene sizes and oxidation states. Each subsection contains the description of the dynamics for every different graphene sheet initial position with respect to the lipid vesicle.

6.1. LARGE AND NON-OXIDIZED GRAPHENE SIMULATIONS

This subsection reports the results for the large and non-oxidized graphene simulation set. For each of the simulations a different system evolution path is found out. First, the corner initial setting is considered (Figure 8a). As it is shown in the figure, the vesicle wets the graphene sheet in the very early of the simulation, 12ns out of 1000ns (Figure 8b). The graphene sheet gets bowed in the vesicle direction and quickly gets absorbed. During the whole simulation, the graphene sheet tilts from the initial position and pierce the vesicle until the complete wetting. The piercing process is slower compared to initial interaction stage. It could be observed because it spends almost the whole simulation to take place. The graphene layer takes an embedded configuration to maximize the contact with the lipid tails. As it is shown in the last frame (Figure 8c), the inner sphere formed by the lipid polar heads is disrupted. This fact indicates that the lipids in both parts of the bilayer are interacting with the graphene. This disruption does not enable the water-graphene contact.

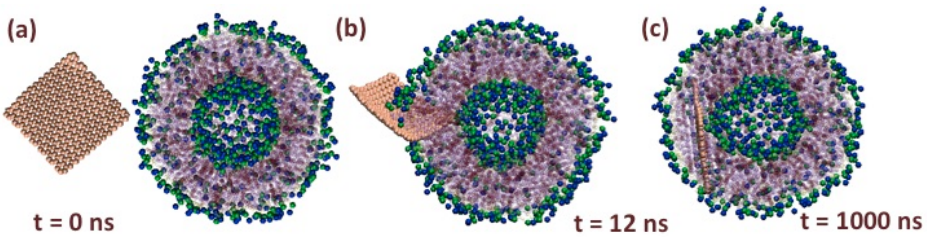

Figure 8. Corner setting dynamics for the large and non-oxidized graphene sheet.

A different evolution path is found for the edge initial configuration (Figure 9a). As it is shown in (Figure 9b), the wetting phenomenon is now taking place trough the graphene edge. The initial interaction is also as quick as in the corner setting case. Moreover, the same graphene plane bowing is shown. Sequentially, the graphene displaces the vesicle polar heads and strengthens the contact with the inner lipid sphere. In this simulation, the graphene sheet does not pierce inside the vesicle but only wets the outer surface of it. It is observed that the graphene sheet substitutes the lipids from the outer layer creating a monolayer (Figure 9c). Thus, the interaction mechanism is clearly different from the corner setting because, in this case, the graphene sheet is partially in contact with the water media in the largest part of the dynamic.

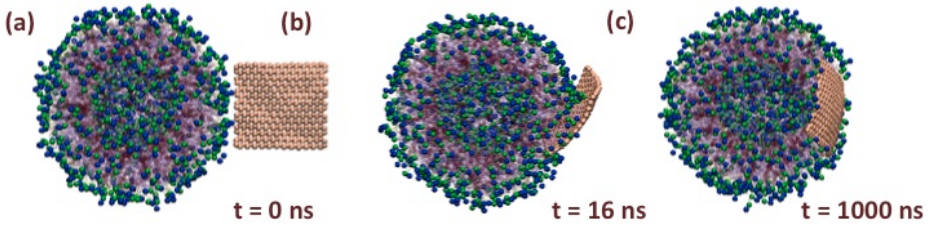

Figure 9. Edge setting dynamics for the large and non-oxidized graphene sheet.

On the other hand, for the face-placed initial configuration dynamics (Figure 10a), none graphene-vesicle direct contact has been captured along the simulation. As it is shown in (Figure 10b), the graphene sheet is twisted but not preferentially bowed towards the vesicle. But after some time, the graphene's corners are clearly tilted outward (Figure 10c), into the aqueous media direction. From 36ns until the end of the simulation the graphene sheet keeps pretty close moving around the vesicle, which means that there exists a slight interaction, despite any noticeable direct contact is registered.

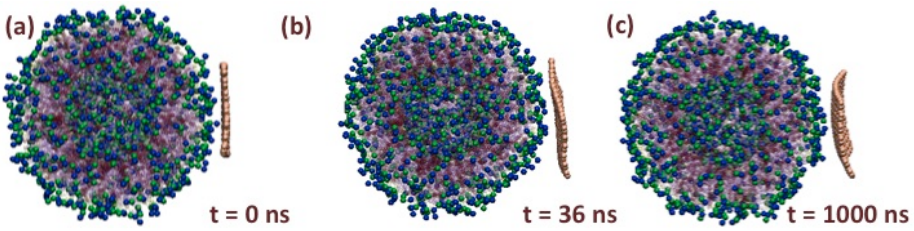

Figure 10. Face setting dynamics for the large and non-oxidized graphene sheet.

Finally, the inside-placed initial condition dynamics are shown. As noted in Figure 11a, the initial configuration diverges with respect to the other settings. Since the graphene is larger than the inner vesicle volume, it exists a direct contact between the vesicle and the graphene sheet from the initial position, while in the others does not. As it is shown in Figure 11b, the system evolves into the inner sphere division path. Despite, the lipids move preferentially to one of the inner water drops and the graphene sheet is turned away. However, a small amount of lipids hold in the smaller drop and the system get aground in this configuration, preventing the graphene sheet to get completely wet by the bilayer lipid tails. The image at Figure 11c shows up the first moment where this lasting state is reached.

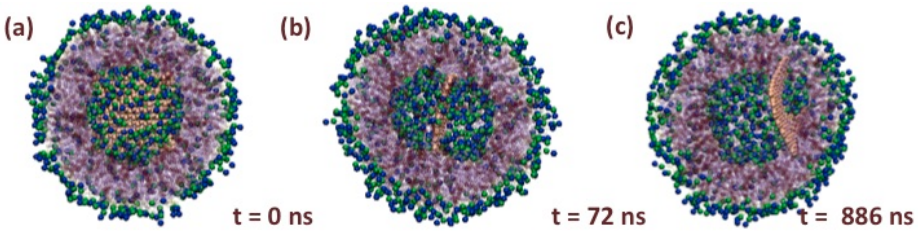

Figure 11. Inside setting dynamics for the large and non-oxidized graphene sheet.

6.2. LARGE AND OXIDIZED GRAPHENE SIMULATIONS

In this section, the MD results for the large and oxidized graphene are described. A shorter number of different outcomes have been found with respect to the initial settings. There exist two initial conditions that follows the same evolution path and, generally, the dynamics are also quite similar to the non-oxidized and corner-placed case. For example, if the corner initial setting (Figure 12a) is considered, the results show up the same interaction mechanism than the corner configuration in the non-oxidized sheet, although reaching this configuration takes longer. Another important feature is related with the interaction between the lipid tails and the graphene sheet. The results in the non-oxidized graphene case show that contact with water is avoided, but appears to be different in this case (Figure 12c). This is basically noticeable in the final state configuration: on the non-oxidized case, graphene disturbs the inner polar head sphere but prevents contact with the water inside it, while a certain graphene-water contact is clearly detected in the oxidized case.

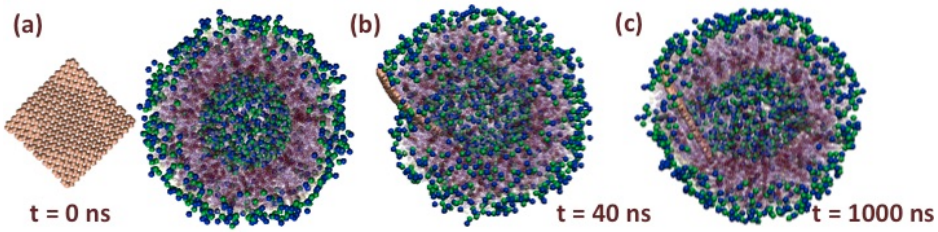

Figure 12. Corners setting dynamics for the large and oxidized graphene sheet.

On the other hand, the edge-placed dynamics (Figure 13a) evolution is clearly different with respect to the non-oxidized situation. In this simulation, the graphene sheet enters into the vesicle, while it wets the outer surface in the non-oxidized case. With respect to dynamics path, it is pretty similar to the oxidized graphene in the corner setting. However, there exist slight differences between them. For example, the invested time to reach the Figure 13b configuration is now shorter. Moreover, the wetted graphene surface area in the last frame (Figure 13c) is also bigger in this simulation. This fact suggests that, compared to the oxidized graphene in the corner setting, this configuration is still stationary, not in the final equilibrium state.

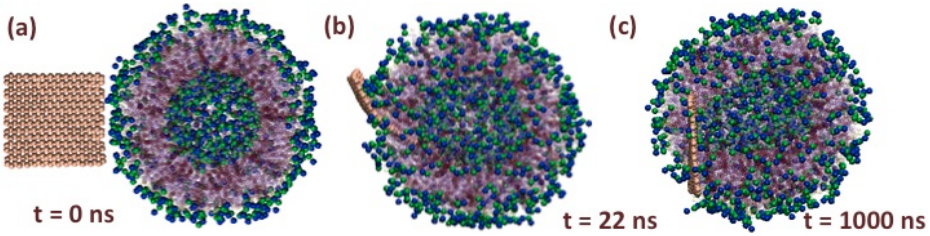

Figure 13. Edge setting dynamics for the large and oxidized graphene sheet.

In the face-placed case (Figure 14a), a large part of the simulation the graphene sheet moves around the vesicle without any direct contact with the vesicle. Nevertheless, the graphene bowing is now looking inward. Eventually, it wets the surface at 474ns (Figure 14b), which is the first moment where a direct graphene-vesicle contact is captured. At this moment, the graphene-vesicle contact increases, until a certain point where graphene push the lipid polar heads away, forming a monolayer (Figure 14c). In this arrangement, the lipid tails of the monolayer still keep contact with graphene.

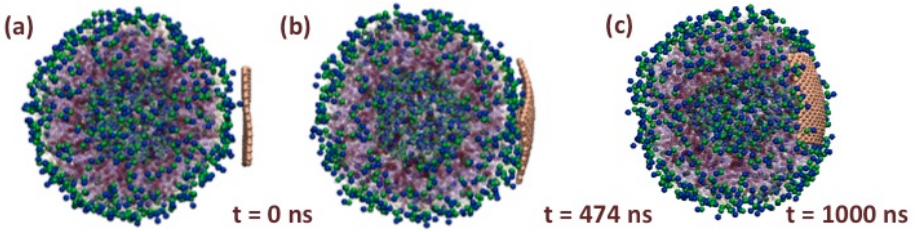

Figure 14. Face setting dynamics for the large and oxidized graphene sheet.

Finally, the inside initial setting (Figure 15a) is described. As it is mentioned in previous inside setting, initial graphene-vesicle direct contact must take place due to the graphene size with respect to the inner sphere diameter. During the simulation, the system remains stacked at the initial configuration just until the half of it. At this point, the vesicle lipids preferentially wets one of the graphene edges (Figure 15b) making the system evolve into the complete wetting. Such process takes from 400ns until 700ns. The final state (Figure 15c) shows up a configuration where the graphene layer is almost perpendicular to the vesicle surface while in the other cases it stayed parallel. This configuration lasts until the end of the simulation, which means that is stable at relative large time-scales.

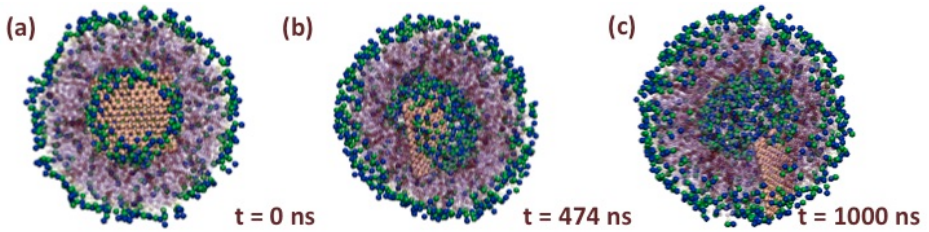

Figure 15. Inside setting dynamics for the large and oxidized graphene sheet.

6.3. SMALL AND NON-OXIDIZED GRAPHENE SIMULATONS

In this section the non-oxidized and smaller graphene simulations are described. Two different outcomes have been registered in terms of the evolution paths. In this graphene size and setting, the simulation passes through three clearly differentiated states. The first one is highlighted for the initial contact process. This state stays only for few picoseconds and is characterized for the graphene tilting in order to interact with the vesicle preferentially from its face. It ends up in a lasting state where the vesicle wets the graphene in a similar way to the one shown in Figure 16b. This configuration could be wrongly associated to the one shown in the bigger graphene cases. Instead, this dynamics does not show a total lipid displacement but a lipid's polar head displacement. The graphene is in direct contact with the lipid polar tails of the outer layer, but not with the inner one. After 100ns, the graphene sheet suddenly gets absorbed placing itself perpendicular to the bilayer of the lipid vesicle (Figure 16c). This previously described situation stays from 102ns until the end of the simulation.

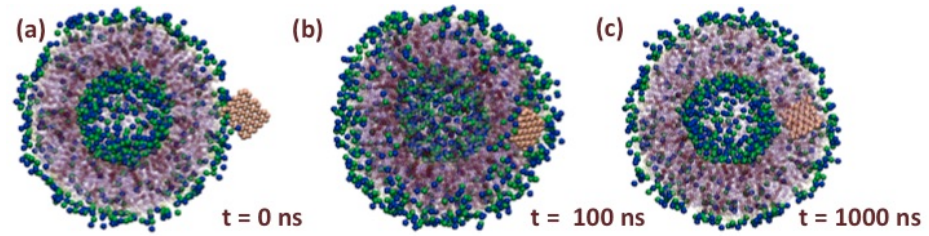

Figure 16. Corner setting dynamics for the small and non-oxidized graphene sheet.

In the face setting case (Figure 17a), the system dynamics also pass through three different states. In the first one, the graphene sheet gets tilted and interacts with the vesicle.

Sequentially, the vesicle wets the graphene sheet from its edge and finally gets adsorbed in the surface. This process takes place in few nanoseconds and remains moving around the surface plane until 134ns (Figure 17b). After this moment, the graphene sheet suddenly gets absorbed and stands perpendicular to the vesicle plane. From 140ns the graphene lasts as shown in Figure 17c until the end of the simulation without any qualitative difference. At this conformation, the graphene surface is in contact with both inner and outer tails of the vesicle lipids.

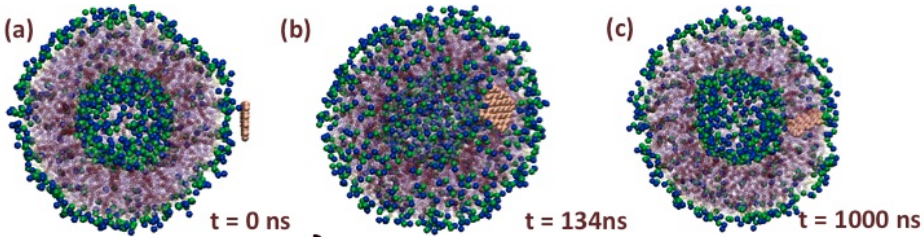

Figure 17. Face setting dynamics for the small and non-oxidized graphene sheet.

In the edge setting (Figure 18a), the dynamics is slightly different to the other ones because the system does not show an intermediate state where the lipid's polar heads are displaced before piercing the vesicle. In contrast, a direct absorption is registered (Figure 18a). The graphene sheet flips around itself interacting with the vesicle from its corner. The graphene does not get adsorbed perpendicular to the vesicle but gets tilted. This process quickly takes place in 4ns. Once the graphene sheet is absorbed it stays perpendicular to the vesicle surface on a lasting state that remains until the end of the simulation (Figure 18c).

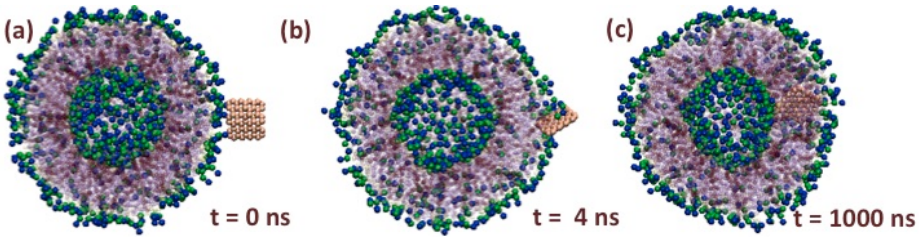

Figure 18. Edge setting dynamics for the small and non-oxidized graphene sheet.

Finally, the same dynamics has been registered for the inside setting (Figure 19a). The graphene sheet is directly absorbed into the vesicle (Figure 19b) without passing through an adsorbed conformation. Nevertheless, in this case the graphene sheet takes contact from its

edge, instead of its corner. Moreover, one of the main differences with respect to the compared one is the gap time from the initial state until the absorption. In the edge setting, it takes 4ns to establish direct graphene-vesicle interaction, while in this case it takes approximately 24ns. Once absorbed it holds on the same configuration until the end of the simulation (Figure 19c), as it is commented for all the simulations discussed so far.

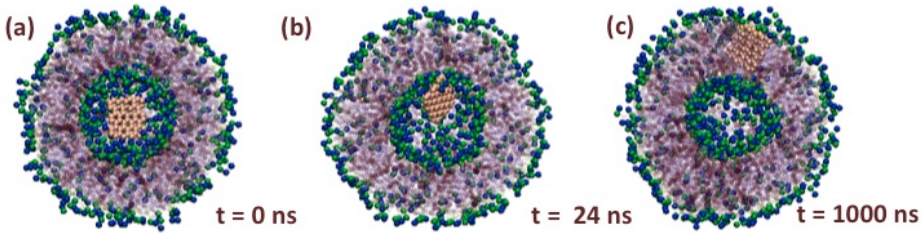

Figure 19. Inside setting dynamics for the small and non-oxidized graphene sheet.

6.4. SMALL AND OXIDIZED GRAPHENE SIMULATIONS

For the small and oxidized corner, edge and face simulations are jointly discussed. The figure used in this section belongs to the corner setting (Figure 20a) but the representation for all three is quite similar. The MD dynamics for this group consist on an initial contact between the graphene sheet and the lipid vesicle. The contact is always taking place from an edge relative position (Figure 20b). Thus, the initial configurations that have different initial configuration quickly evolve to the edge one in a few nanoseconds. Nevertheless, the edge contact is never happening perpendicularly to the vesicle but requires a certain contact angle.

After the initial contact, the graphene sheet gets adsorbed on the vesicle surface (Figure 20c). Similarly to all the small-size graphene cases, only the polar lipid heads are displaced but the interaction is still taking place with the outer layer. The graphene sheet holds in this lasting state, moving around the vesicle, without piercing it.

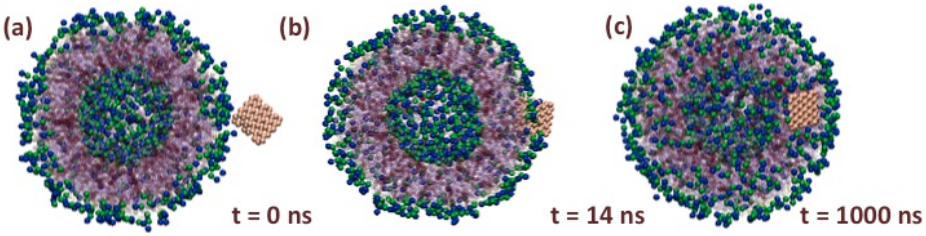

Figure 20. Corner, edge and face setting dynamics for the small and oxidized graphene sheet. The pictures are taken form the corner setting.

In turn, in the inside setting (Figure 21a), the graphene sheet moves around the inner water media for a while. At 12ps, it suddenly makes direct contact with the lipid polar heads and get wet without an intermediate adsorption state. The graphene layer overcomes the inner polar sphere (Figure 21b) and holds perpendicular to the vesicle surface. It lasts moving around the vesicle until the end of the simulation (Figure 21c). This initial setting shows a completely different outcome compared to the rest of graphene placements in this section.

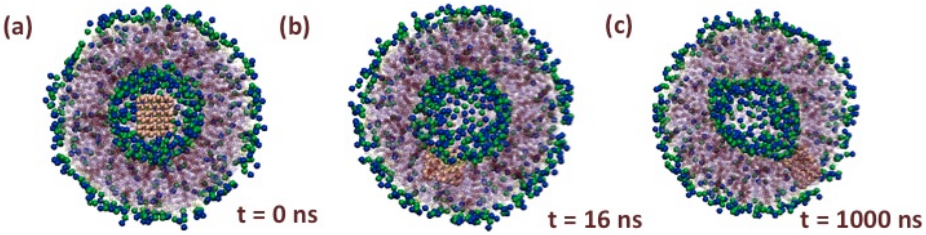

Figure 21. Inside setting dynamics for the small and oxidized graphene sheet.

6.5. GRAPHENE ON PLANAR BILAYERS

The dynamics described here for small graphene sheets are different compared to the behaviour reported recently [12-14] for a MD study where graphene interacts with planar bilayers. In these works the bilayer does also absorb the graphene sheet and get in contact with the last beads of the lipid tails. In turn, the graphene sheet stays parallel to the lipid bilayer instead of perpendicular to the surface plane. Therefore, it is reasonable to think that some of the simulation conditions (planar vs. curved) are different with respect to the reported ones.

In order to compare these results with the reported ones, some extra calculations have been performed. The first of them consist on testing another initial geometry. This one place the graphene sheet in the final structures reported in the literature, embedded inside by the vesicle. These simulations have been performed for both oxidation states of the smaller graphene sheets. On the other hand, a planar lipid bilayer was built in order to test if the simulation conditions properly reproduce the reported results. In this case, the graphene is also initially placed in the middle of the lipid bilayer to test its stability.

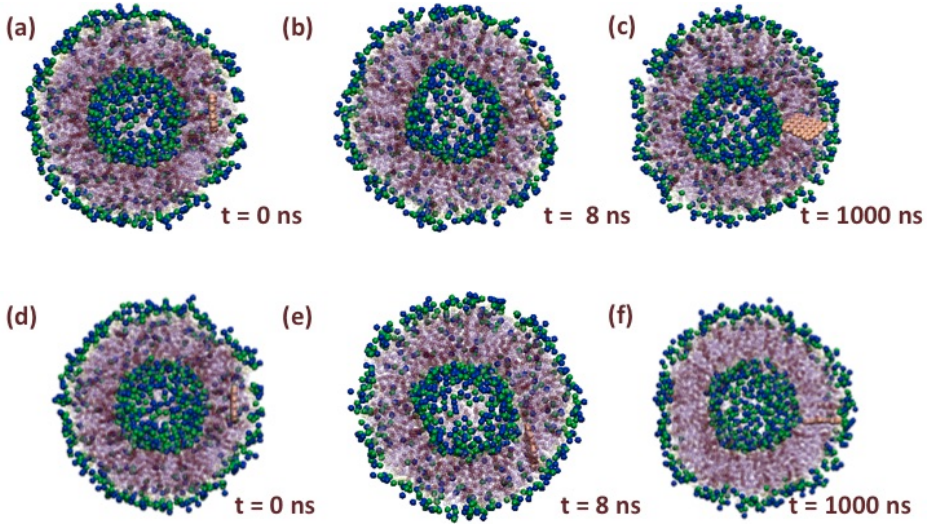

Figure 22. The graphene is initially placed within the vesicle. The frames (a-c) correspond to the non-oxidized graphene sheet. The frames (d-f) correspond to the oxidized graphene sheet.

In the vesicle case, the system evolved into the same final structure for both oxidation states. The initial structure is the one shown in Figure 22a and Figure 22d. Starting from this configuration, the graphene sheet quickly turns and takes the perpendicular conformation (Figure 22c and Figure 22f) reported in the previous sections. Moreover, the process is quite fast, because it takes place in the first 8ns (Figure 22b and Figure 22e).

Unlike the previous dynamic study, graphene stays parallel to the bilayer surface when it is planar. A lateral movement could be observed for both oxidation states (Figure 23). During the simulation, graphene moves among the lipid bilayer along the XY plane. Time to time, it tilts but

quickly returns to the initial horizontal configuration. This lateral movement is more common for the oxidized graphene sheet than for the non-oxidized one.

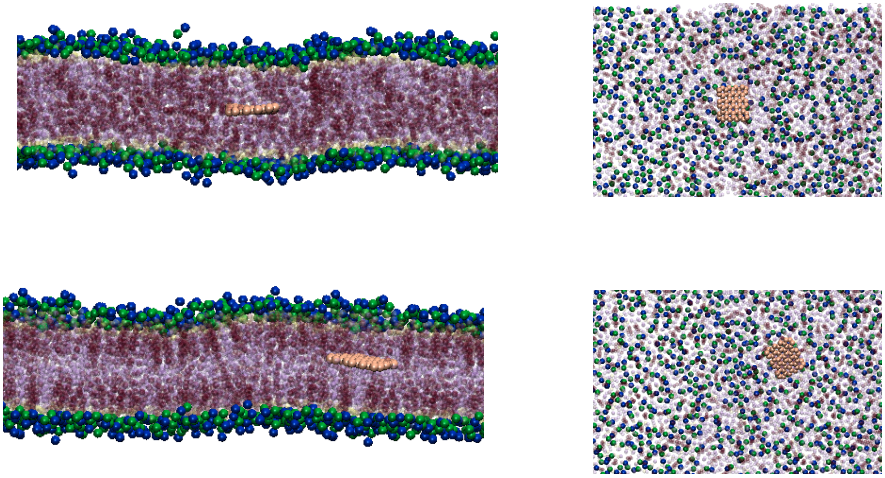

Figure 23. Different views of the non-oxidized graphene simulations within a planar bilayer. Top: different views o the initial configuration. Bottom: different views of the final configuration. Notice that the graphene moves around the vesicle plane.

7. DISCUSSION

In this section, the different results obtained in the MD simulations are discussed. The whole studied system contains a wide range of variables, such as oxidation state, relative position or the graphene sheet size. Therefore, it is difficult to obtain a general description of the system details with such a reduced number of simulations. However, some tendencies could be figured out from the computational experiments.

One of the main important trends is the one related with the initial graphene orientation. On the one hand, the simulations show that the initial relative position changes the evolution path for the large-size graphene sheets. For example, four different evolution paths are observed out of four different initial relative positions in the large and non-oxidized graphene simulations. The simulations might be classified in two different situations with respect to the final configuration for the whole large graphene sheets dynamics.

The different situations are determined by the number of atoms that simultaneously interacts with the vesicle in the initial contact. For example, if the graphene sheet interacts through the corner only few atoms of the whole graphene sheet directly contact the vesicle at the same time (Few-particle initial contact). On the other hand, if the graphene sheet is face-placed all the particles are directly in contact with the vesicle (Many-particle initial contact). Those are the limit cases, but edge setting and inside setting would be in few-particle initial contact and many-particle initial contact interaction groups, respectively. According to this classification, the simulations collected in the few-particle initial contact normally pierce the vesicle, while an adsorption, or another final state process, is registered for many-particle initial contact ones.

The main point to justify this behaviour is closely related to the space needed to penetrate the vesicle. When the large graphene sheet pierces it, a large number of lipid particles must move in order to room the entering sheet. Thus, if the displacement is done in a step-by-step process, graphene could reorient in each of those steps and finally pierce the vesicle. Therefore, in the few-particle initial contact configurations the graphene sheet generally penetrates it, because the piercing is a stepwise process. In turn, any rearrangement is

sterically forbidden when all the atoms pierce the vesicle simultaneously, because a large lipid displacement should happen. Such process take place at the many-atom initial contact set.

The grouping done until the moment does generally make sense without considering the oxidation degree of the graphene sheet. Nevertheless, the piercing process does more often appear in the oxidized cases. This fact could be understood attending to the activation energy of each. The first interaction between the vesicle lipids and the graphene sheet takes places trough the contact with the lipid polar heads. Those ones are hydrophilic chemical groups, so that, they preferentially interact with other hydrophilic particles. Taking the chemical graphene nature into account, the interaction is pretty much favourable when it is oxidized. Thus, both few-particle initial contact cases can overcome the energy barrier and interact with vesicle lipid tails. In turn, the non-oxidized graphene sheet does not show such strong contact with the lipid's polar heads. Then, the energy barrier becomes larger in this case, making any configuration but the corner one pierce the vesicle. Derived by this reasoning, the piercing process is highly more sensitive to the initial configuration when the graphene sheet is non-oxidized.

The initial conditions belonging to the many-atom initial contact set do also agree with the activation energy reasoning. For example, the vesicle finally wets the graphene in the oxidized and face-placed case. However, none direct contact is registered in the non-oxidized graphene sheet. Intuitively, the activation energy increases when the atoms that simultaneously try to pierce the vesicle do also increase.

In the smaller graphene cases the initial configuration does not determine the graphene dynamics, because the many-atom initial contact simulations do also pierce the vesicle. There are two valid arguments to justify this behaviour. The first one consists on following the same reasoning done above. In these terms, rooming the graphene sheet does not need a large lipid rearrangement in the smaller graphene sheets. Thus, it is easier to pierce the vesicle; even this contact implicates all the atoms simultaneously. The second argument lies on the thermal fluctuations. In every simulation the water particles stumble upon the graphene sheet making these to move around the solution. In the larger graphene cases, this movement does not highly affect, because it is more difficult to move a large body. Nevertheless, in the small-size graphene sheets it is easier and the thermal fluctuation effect appears. This fact simply means that small graphene sheets can randomly rotate and tilt before interacting the vesicle, which makes the relative positioning ineffective.

However, the thermal fluctuation reasoning does not justify the differences in the interaction paths between oxidized and non-oxidized cases in the smaller graphene sheets. For example, the graphene sheets always end up piercing the vesicle in the non-oxidized situation but in the oxidized case a lasting adsorption is found out. For this reason, the graphene oxidation effect after the adsorption must be inquired.

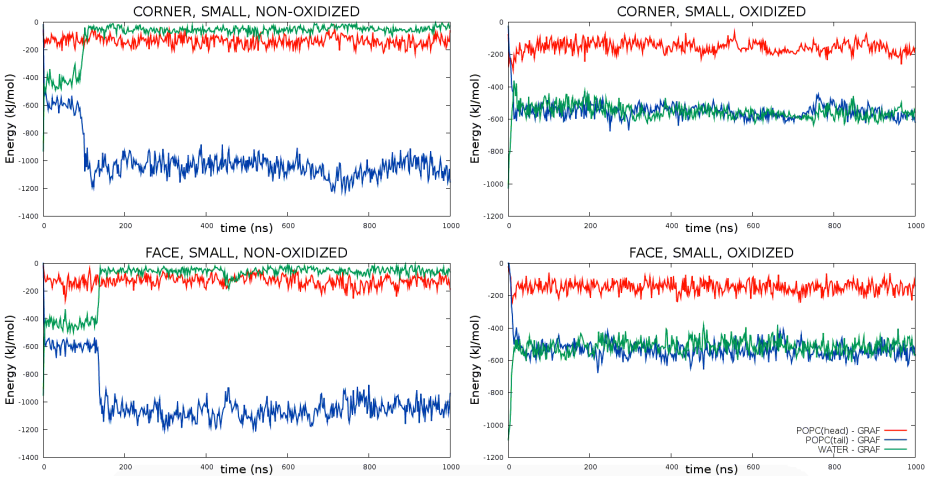

Figure 24. Small graphene sheets interaction energy with POPC heads (red), POPC tails (blue) and water (green). Left-placed plots correspond to non-oxidized graphene sheets and right-placed plots correspond to oxidized graphene sheets.

In Figure 24, the interaction energy profiles between the POPC (polar head), POPC (apolar tail) and water with the graphene sheet are represented. Different plots are collected in the figure, which collect the cases where the smaller graphene sheets adsorb the surface. Several differences are appreciated between them all. The main important is related with the differences in the POPC (apolar tail)-graphene and water-graphene interaction. In the non-oxidized case, stronger interaction energy between POPC (apolar tail) and graphene is registered with respect to the graphene-water one. However, the same value is almost obtained in the oxidized case. This energy difference is qualitatively understandable: the oxidized sheets maintain a stronger interaction with water than the non-oxidized ones. Simultaneously, the oxidation reduces the interaction energy of the graphene sheet with POPC (apolar tail). Then, the oxidized graphene

exposition to water is, in balance, more favourable. For this reason, the oxidized graphene sheet lasts in the adsorption state while it pierces the vesicle in the non-oxidized case.

Nevertheless, the inside initial setting does actually pierce the vesicle, in the small-size and oxidized graphene sheets. This particular outcome provides useful information to observe the curvature effects and also helps to justify the metastability of the rest of the oxidized graphene sheets. The different interaction path lies in the fact that vesicle curvature in the inner layer is higher than in the outer one. Thus, the adsorption in the outer layer does not require a graphene bowing to take place. In turn, the graphene sheet must get bowed in order to get a complete face contact with the inner layer, preferring to directly pierce the vesicle instead.

Moreover, comparing the energy profile of the inside setting with respect to the rest of them (Figure 25), helps to analyse which final state is lower in energy: the POPC (apolar tail)-graphene interaction is several times stronger when the graphene pierce the vesicle than in the adsorption state. Then, the metastability of the adsorption state is confirmed.

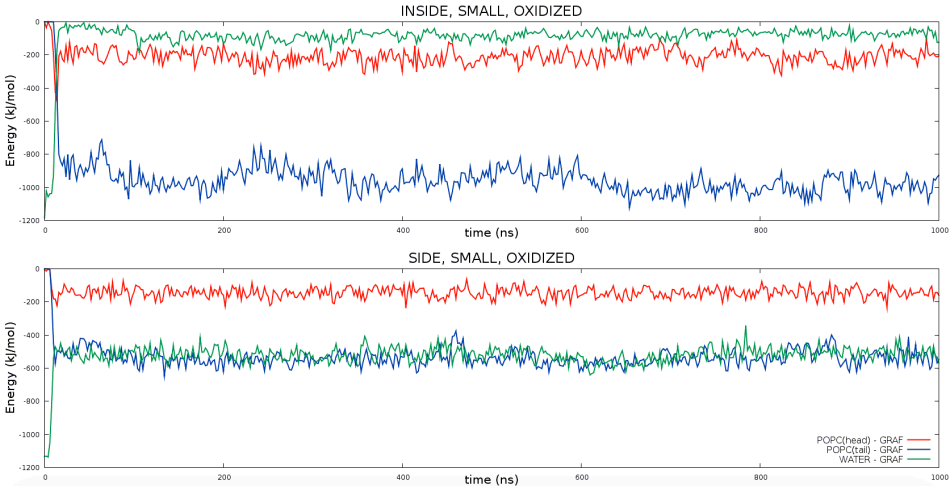

Figure 25. Small graphene sheets interaction energy with POPC heads (red), POPC tails (blue) and water (green). Top: inside initial setting; Bottom: side initial setting

In both non-oxidized and oxidized inside-placed cases the piercing process appear in a strange path. However, there is an interesting feature in the oxidized case that helps to extrapolate how the system would evolve at much larger times of simulation, for the rest of

large-size and oxidized graphene cases. The energy of the final state configuration of the inside-placed could be compared with the same graphene sheet in the corner-placed or edge-placed cases (Figure 26). Then, it is noticeable that the final step interaction between the POPC tails and the graphene in the inside configuration is much lower than in the rest of cases. This means that the corner or edge cases final state is more stable. Therefore, the corner-placed or edge-placed dynamics would surely not evolve into a perpendicular configuration. The same argument does also work comparing the pierced cases with the ones forming a monolayer.

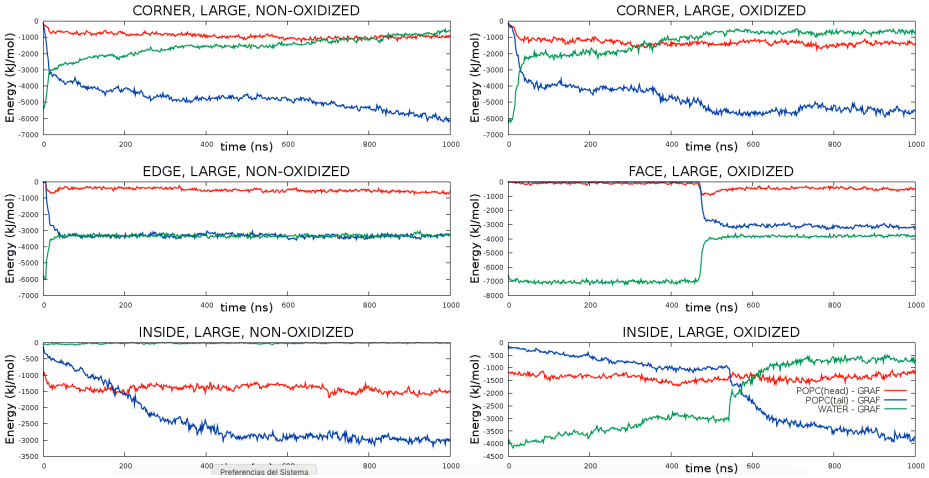

Figure 26. Large graphene sheets interaction energy with POPC heads (red), POPC tails (blue) and water (green). Left-placed plots correspond to non-oxidized graphene sheets and right-placed plots correspond to oxidized graphene sheets.

The combination of both energy-based and steric hindrance reasoning can be jointly applied to large and non-oxidized graphene sheets. In this case, the initially edge-placed simulation shows a displacement of the lipids of the outer layer formation, while graphene pierce the vesicle in the corner case. Again, the number of atoms that may simultaneously penetrate the vesicle in the edge-placed configuration is larger than in the corner one. Then, in this case, the energy barrier is higher than in the oxidized case, so the piercing process does not happen. Such fact is justified also by looking at the energy profile (Figure 26).

Another important feature to take into account is the final pierced state, for the vesicles in the small graphene sheets, with respect to the ones found in the literature. As it appears in the

MD, the graphene sheet holds perpendicular to the surface plane when it pierces the vesicle. In the other hand, considering a planar lipid bilayer turns out to a parallel graphene configuration, in all the cases. This fact could be understood by the graphene bowing reasoning provided above. In order to stay totally within the vesicle, the graphene sheet must get bowed. As it is a stiff material, the energy gain on stay parallel to the vesicle bilayer plane does not compensate the deformation energy.

8. FURTHER PERSPECTIVES: GRAPHENE-MEDIATED VESICLE FUSION

Vesicle fusion is an important issue for processes such as intracellular trafficking, neurotransmitter releases or for the viral infectivity. The vesicle fusion process is thermodynamically favoured, because this process reduces the both membrane and surface tension. However, lipid vesicles are charged supramolecular complexes, and they repeal each other making the vesicle fusion a really slow process. In nature, proteins bring the vesicles in a closer position and normally mediate the vesicle fusion. Some computational studies investigated the vesicle fusion path [19-21] and also demonstrated that adding Ca^{2+} ions in the media could drive this process [22], if the vesicle lipids are negatively charged. Those ions reduce the vesicle effective repulsions and the fusion become faster. However, the graphene-mediated vesicle fusion had been never tested. In this section, the graphene effect with respect to this process is proved.

Here, a MD simulation of two identical vesicles connected by a graphene sheet is performed. In this case, a 12x13 coarse-grained graphene sheet has been used. Moreover, the simulations have been done for both oxidized and non-oxidized case. The registered results for the graphene effect in a single-vesicle system show that the corner initial setting is the most appropriate relative position for the vesicle piercing process. This fact might make this setting the most appropriate one for the fusion process to take place. In the initial configuration, the graphene sheet has been placed this way but wetting both graphene vesicles in the initial topology (Figure 27a).

The vesicle fusion for the non-oxidized graphene sheet evolved as it is shown in Figure 27. At the first 16ns the first contact between vesicles is registered (Figure 27b). From this point on, the contact gets stronger (Figure 27c) until the moment where lipid polar heads are totally displaced and the inner polar sphere also get hemifused (Figure 27d). From this moment until the end of the simulation, a spherical arrangement is recovered, ending in Figure 27e configuration.

Moreover, the key role of the oxidation degree has been also noticed, because the simulation where an oxidized graphene is used evolved in a completely different path. In this last one, the graphene sheet preferentially interacts with one of the vesicles that finally absorb it. Thus, both vesicles remains moving around the simulation and box repealing each other, making the graphene presence useless to mediate the vesicle fusion.

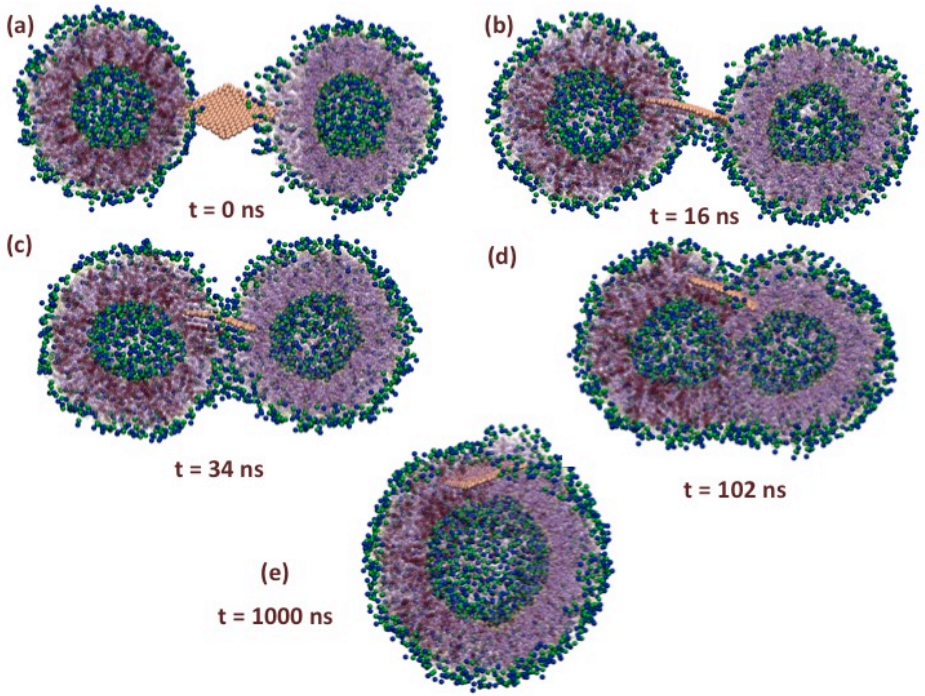

Figure 27. Graphene-mediated vesicle fusion using a 12x13 non-oxidized graphene sheet. In the left→right and top→down pictures the evolution of the system is graphically described.

9. CONCLUSIONS

The relative orientation of graphene with respect to the vesicle affects the evolution path in the cases where the graphene sheet is large-sized. In turn, such effect is not noticed for the small-sized graphene sheets, appearing to be masked by thermal fluctuations.

According to the larger graphene sheets, the piercing process does take place when the lipid apolar tails room the graphene sheet throughout a stepwise process. However, a metastable state is reached when the initial contact involves all the graphene atoms simultaneously.

The graphene size affect to the total conformation of the vesicle-graphene system in the cases where an adsorption is registered. For the large-sized graphene sheets, the interaction of graphene with the vesicle produces a displacement of the lipids forming the outer layer. In turn, only the polar heads are displaced in the small-sized graphene sheets.

The oxidation state of graphene modifies its stability in water and determines the final state of the graphene-vesicle interaction in the small-sized cases. Oxidized graphene sheets metastablely remains adsorbed in the surfaces while non-oxidized sheets eventually pierce the vesicle.

The lipid bilayer curvature determines the relative position of small-sized graphene sheets. A perpendicular setting is registered for the vesicle simulation cases. In turn, a parallel relative orientation is registered in the planar lipid bilayer cases. The final configuration of the graphene sheet with respect to the vesicle apparently changes according to the apolar-apolar interaction energy and the deformation energy of the graphene sheet.

Totally embedded configurations are more stable than neither adsorbed nor perpendicular final states. The metastability of these last configurations has been determined comparing the energy profiles.

A new graphene-mediated vesicle fusion process has been registered. The process seems to be sensitive to the oxidation of the graphene sheet. However, a larger mapping of graphene sizes and orientations might be performed in order to properly understand this process.

10. REFERENCES AND NOTES

1. Geim, A. K.; Novoselov, K. S. The Rise of Graphene. *Nat. Mater.* **2007,** *6*, 183−191.
2. Wang, K.; Ruan, J.; Song, H.; Zhang, J.; Wo, Y.; Guo, S.; Cui, D. Biocompatibility of Graphene Oxide. *Nanoscale Res. Lett.* **2011,** *6*,8-16.
3. Mannelli, I.; Sagués, F.; Pruneri, V.; Reigada, R. Lipid Vesicle Interaction with Hidrophobic Surfaces: A Coarse-Grained Molecular Dynamics Study. *Langmuir* **2016,** *32*, 12632-12640.
4. Mannelli I.; Reigada, R.; Suárez, I.; Janner, D.; Carrilero, A.; Mazumder, P.; Sagués, F.; Pruneri, V.; Lakadamyali, M. Functionalized Surfaces with Tailored Wettability Determine Influenza A Infectivity. *ACS Appl. Mater. Interfaces* **2016,** *8*, 15058-15066.
5. Willems, N.; Urtizberea, A.; Verre, A. F.; Iliut, M.; Lelimousin, M.; Hirtz, M.; Vijayaraghavan, A.; Sansom, M. S. P. Biomimetic Phospholipid Membrane Organization on Graphene and Graphene Oxide Surfaces: A molecular Dynamics Simulation Study. *ACS Nano* **2017,***11,*1613-1625.
6. Huang, P. J.; Wang, F.; Liu, J. Liposome/Graphene Oxide Interaction Studied by Isothermal Titration Calorimetry. *Langmuir* **2016,** *32*, 2458-2463.
7. Liu, X.; Chen, K. L. Interactions of Graphene Oxide with Model Cell Membranes: Probing Nanoparticle Attachment and Lipid Bilayer Disruption. *Langmuir* **2015,** *31*, 12076-12086.
8. Frost, R.; Svedhem, S.; Langhammer C.; Kasemo B. Graphene Oxide and Lipid Membranes: Size-Dependent Interactions. *Langmuir* **2016,** *32*, 2708-2717.
9. Sanchez, V. C.; Jachak, A.; Hurt, R. H.; Kane, A. B. Biological Interactions of Graphene-family Nanomaterials: an Interdisciplinary Review. *Chem. Res. Toxicol.* **2014,** *25*, 15−34.
10. Bianco, A. Graphene: Safe or Toxic? The Two Faces of the Medal. *Angew. Chem.* **2013,** *52*, 4986−4997.
11. Dryer, D. R.; Park, S.; Bielawski, C. W.; Ruoff, R. S. The Chemistry of Graphene Oxide. *Chem. Soc. Rev.* **2010,** *39*, 228-240.
12. Titov, A. V.; Král, P.; Pearson, R. Sandwiched Graphene-Membrane Superstructures. *ACS Nano* **2010,** *4*, 229-234.
13. Wang, J.; Wei, Y.; Shi, X.; Gao, H. Cellular Entry of Graphene Nanosheets: The Role of Thickness, Oxidation and Surface Adsorption. *RSC Advances* **2013,** *3*, 15776-15782.
14. Yinfeng, L.; Hongyan, Y.; von dem Bussche, A.; Creighton, M.; Hurt, R. H.; Kane, A. B.; Gao, H. Graphene Microsheets Enter Cells Through Spontaneous Membrane Penetration at Edge Asperities and Corner Sites. *P. Natl. Acad. Sci. USA* **2013,** *110*, 12295-12300.
15. Marrink, S. J.; Risselada, H. J.; Yefimov, S.; Tieleman; D. P. de Vries, A. H. The MARTINI Force Field: Coarse Grained Model for Biomolecular Simulations. *J. Phys. Chem B* **2007,** *111*, 7812-7824.
16. Ruiz, L.; Xia, W.; Meng, Z.; Keten, S. A Coarse-Grained Model of the Mechanical Behavior of Multi-Layer Graphene. *Carbon* **2015,** *82*, 103-115.
17. Berendsen H. J. C.; van der Spoel, D.; van Drunen, R. GROMACS: A Message-Passing Parallel Molecular Dynamics Implementation. *Comput. Phys. Comm.* **1995,** *91*, 43-56.
18. van der Spoel, D.; Lindhal, E.; Hess, B.; van Buuren, E.; Apol, E.; Meulenhoff, P. J.; Tielman, D. P.; Sijbers, A. L.; Feenstra, K. A.; van Drunen, R.; Berendsen, H. J. C. Gromacs User Manual Version 4.5.4, www.gromacs.org **2010,** p45.
19. Kasson, P. M.; Lindahl, E.; Pande, V. S. Atomic-Resolution Simulations Predict a Transition State for Vesicle Fusion Defined by Contact of a Few Lipid Tails. *PLoS Comput. Biol.* **2010,** *6*, e1000829.

20. Grafmüller, A.; Schillcock J.; Lipowsky, R. The Fusion of Membranes and Vesicles: Pathway and Energy Barriers from Dissipative Particle Dynamics. *Biophys. J.* **2009,** *96*, 2659-2675.
21. Marrink S. J.; Mark, A. E.; The Mechanism of Vesicle Fusion as Revealed by Molecular Dynamics Simulations. *J. Am. Chem. Soc.* **2003,** *125*, 11144-111145.
22. Tsai, H. G.; Chang, C.; Lee, J. Multi-Step Formation of a Hemifusion Diaphragm for Vesicle Fusion Revealed by All-atom Molecular Dynamics Simulations. *Biochimica et Biophysica Acta* **2014,** *1838,* 1529-1535.

11. ACRONYMS

POPC: 1-palmitoyl-2-oleoyl-sn-glycero-3-phosphocholine

MD: Molecular Dynamics

CGMD: Coarse-grained Molecular Dynamics

GO: Graphene Oxide

GROMACS: Groningen Machine for Chemical Simulations

FORTRAN: Formula Translation

PBC: Periodic Boundary Conditions